Available online at www.sciencedirect.com
ScienceDirect
Carbohydrate Polymers 68 (2007) 146–158
Carbohydrate Polymers
www.elsevier.com/locate/carbpol

Physical properties of starch nanocrystal-reinforced pullulan films

Eleana Kristo, Costas G. Biliaderis *

Laboratory of Food Chemistry and Biochemistry, Department of Food Science and Technology, School of Agriculture, Aristotle University, GR-541 24, Thessaloniki, Greece

Received 28 June 2006; received in revised form 19 July 2006; accepted 20 July 2006
Available online 1 September 2006

Abstract

Nanocomposite materials were prepared using sorbitol-plasticized pullulan as the amorphous matrix and an aqueous suspension of starch nanocrystals (prepared by submitting native granules from waxy maize starch to acid hydrolysis at 35 °C) as the reinforcing phase. Wide-angle X-ray diffraction analysis showed an increase of the crystallinity of the composite biopolymer films with increasing of starch nanocrystal content. The water absorption isotherms and kinetics as well as the water barrier properties of nanocomposite films filled with 0–40% (w/w) starch nanocrystals (starch nanocrystals/pullulan + sorbitol) were investigated. The water uptake of pullulan–starch nanocomposites decreased with increasing filler content whereas water vapor permeability (measured at 25 °C and 53/100 relative humidity (RH) gradient) remained constant up to 20% (w/w) and, then decreased significantly with further addition of nanocrystals. The thermo-mechanical behaviour of nanocomposite films was also investigated by means of dynamic mechanical thermal analysis (DMTA) and large deformation mechanical tests (tensile mode). The glass transition temperature (T_g) shifted towards higher temperatures with increasing amount of nanocrystals, which can be attributed to a restriction of the mobility of pullulan chains due to the establishment of strong interactions not only between starch nanocrystals but also between the filler and the matrix. Moreover, the addition of nanocrystals caused strong enhancement of the Young modulus and the tensile strength, but led to a drastic decrease of the strain at break in samples conditioned at different environments (from 43% to 75% RH).
© 2006 Elsevier Ltd. All rights reserved.

Keywords: Pullulan; Edible films; Tensile properties; Thermomechanical analysis; Nanocomposite; Starch crystalline particles; Water permeability; Plasticization

1. Introduction

Nanocomposites are a relatively new class of composites consisting of polymers filled with particles that have at least one dimension in the nanometer range. Because of their very high surface area to volume ratio, nanoparticle incorporation into polymer matrices leads to composites with unique outstanding properties in comparison to their conventional microcomposite counterparts (Smith, Bedrov, & Smith, 2003). The biocompatibility and biodegradability of synthetic materials used in nanocomposite preparation are more limited than those of natural polymers. In this context research has been focused on using natural nanofillers in various polymer matrices. The main advantages of such fillers are their renewable nature, availability, high specific strength, non-abrasive nature that allows easier processing even at high filling levels, biodegradability as well as the relatively reactive surface which can be modified accordingly (Anglès, Salvadó, & Dufresne, 1999; Azizi Samir, Alloin, & Dufresne, 2005). Thus, nanocomposites obtained by incorporation of cellulose, chitin or starch nanocrystals as nanofillers in both synthetic polymeric matrixes (Chazeau, Cavaillé, Canova, Dendievel, & Boutherin, 1999; Dufresne, Cavaillé, & Helbert, 1996; Dufresne & Cavaillé, 1998; Favier, Chanzy, & Cavaillé, 1995a) and biopolymers (Anglès & Dufresne, 2000; Dubief, Samain, & Dufresne, 1999; Dufresne, Kellerhals, & Witholt, 1999; Noshiki, Nishiyama, Wada, Kuga, & Magoshi, 2002) showed desirable improvement of different properties

* Corresponding author. Tel.: +30 2310 991797; fax: +30 2310 471257.
E-mail address: biliader@agro.auth.gr (C.G. Biliaderis).

0144-8617/$ - see front matter © 2006 Elsevier Ltd. All rights reserved.
doi:10.1016/j.carbpol.2006.07.021

e.g., related with mechanical reinforcement and/or water resistance. The outstanding reinforcement reported in nanocomposites is mostly, defined by the nature of the polymer-particle interface (Dionne, Ozisik, & Picu, 2005; Smith et al., 2003; Zhu & Sternstein, 2003) and/or strength of filler–filler interactions leading in the establishment of a particle percolating network (Dubief et al., 1999; Dufresne & Cavaillé, 1998; Favier et al., 1995a; Morin & Dufresne, 2002).

By submitting native starch granules to an extended-time acid hydrolysis at temperatures below the gelatinization temperature, the amorphous regions are rapidly hydrolyzed allowing the separation of crystalline lamellae, which are more resistant to hydrolysis. This procedure is expected to give lamellar structures that would contain linear chains of DP (Degree of Polymerization) 15 and single-branched molecules of DP 25 as determined by molecular sieve chromatography (Robin, Mercier, Charbonnière, & Guilbot, 1974; Biliaderis, Grant, & Vose, 1981) and supported by TEM measurements (Putaux, Molina-Boisseau, Momaur, & Dufresne, 2003). The starch crystalline particles show platelet morphology with a thickness of 6–8 nm. However, individual starch crystallites could hardly be obtained since the starch platelets flocculate and form aggregates (Putaux et al., 2003). Nevertheless, since at least one of the dimensions of aggregates is at the nanometer scale, the term 'nanoparticle' is applicable for starch crystalline particles derived by acid etching of granular starch (Angellier, Molina-Boisseau, Lebrun, & Dufresne, 2005b).

Pullulan is an extracellular microbial polysaccharide produced by the fungus-like yeast, *Aureobasidium pullulans* (Yuen, 1974). It is water-soluble and forms excellent, colourless, transparent and flexible films. The α $(1 \rightarrow 6)$ linkages that interconnect the repeated maltotriose units along the chain are responsible for the flexible conformation and the ensued amorphous character of this polysaccharide in the solid state (Gidley, Cooke, & Ward-Smith, 1993). Being amorphous, pullulan was considered as a suitable matrix to incorporate waxy maize starch nanocrystals (obtained by hydrolysis of native granules with hydrochloric acid) and to study the properties of the resulting nanocomposites as a function of filler content without the intervention of any inherent polymer crystallinity that would make the system more complex. Therefore, this work was focused on processing and characterization of pullulan–starch nanocrystal composites in terms of thermomechanical as well as water sensitivity and moisture barrier properties.

2. Materials and methods

2.1. Materials

Pullulan was a food grade preparation from Hayashibara Biochemical Laboratory, (Okayama, Japan). Inorganic salts (reagent grade) used for adjusting the relative humidity (RH) (saturated salt solutions) were from Merck KgaA (Darmstadt, Germany). Silica gel used as desiccant was purchased from Sigma–Aldrich GmbH (Germany). Waxy maize starch (WAXILUS 200) was kindly supplied by Roquette S.A. (Lestrem, France).

2.2. Preparation of the starch nanocrystals

Starch nanocrystals were prepared by acid hydrolysis of waxy maize starch according to Dufresne et al. (1996). Starch powder (50 g) was mixed with 1 L of 2.2 N HCl (820 mL of water and 180 mL of 36% HCl) and the suspension was stored at 35 °C for 30 days. The suspension was stirred daily to resuspend the starch granules. After the defined period of time the insoluble residues were recovered by multiple washings and repeated centrifugations until acid free using deionized water. An ultrasonic treatment was then employed to ensure better dispersion of nanocrystals in water. The dispersion was refrigerated until used after sodium azide addition to prevent microbial growth.

2.3. Film processing

A film-forming solution was prepared by mixing the appropriate amount of aqueous suspension of starch nanocrystals with aqueous solution of pullulan and addition of sorbitol as plasticizer. The content of starch nanocrystals ranged from 0% to 40% (w/w) (starch nanoparticles/(pullulan + sorbitol)), namely 0%, 3%, 6%, 10%, 15%, 20%, 30% and 40% (w/w), for all the performed tests except DMTA measurements. For DMTA analysis the concentration of filler was restricted to 15% (w/w), because the use of higher filler level to prepare such thick specimens (~1.5 mm) led to brittle materials that were difficult to handle. Sorbitol was used as plasticizer at a constant concentration of 30% (w/w) relative to the total mass of pullulan and sorbitol (Angellier, Molina-Boisseau, Dole, & Dufresne, 2006; Anglès & Dufresne, 2001). The aqueous mixtures were degassed under vacuum to avoid the formation of air bubbles during water evaporation. Then, the preparations were cast in polystyrene plates and evaporated at 35 °C in an oven until the formation of films, which could be easily removed from the plate. Dry films of different thickness depending on the testing procedure, were thus obtained.

2.4. Film characterization

2.4.1. X-ray diffraction

The wide angle X-ray diffraction analysis was performed on unfilled sample, composite films (filled with 6%, 15% and 30%, w/w starch nanocrystals) and powders of native waxy maize starch granules and air-dried starch crystals, after exposure at 100% RH for ~2 h. The samples were attached to specifically made Plexiglas holders and examined with a Philips X-ray generator PW 1830 equipped with a graphite–crystal monochromator and a vertical goniometer PW 1820. The operating conditions for the refractometer were: copper *Ka* radiation, voltage 40 kV, amperage 30 mA, sampling interval time 0.4 s.

2.4.2. Moisture sorption isotherms

Moisture sorption isotherms were determined as previously described by Biliaderis, Lazaridou, and Arvanitoyannis (1999). Film samples (~300 mg) were placed in previously weighed aluminum dishes and dried at 45 °C in an air-circulated oven over silica gel until constant weight. The samples were subsequently kept in desiccators over saturated salt solutions of known RH at 25 °C for 21 days, a time sufficient to reach constant weight and hence practical equilibrium. The moisture content of samples, after storage, was determined by drying at 110 °C for 2 h. The obtained data were fitted to the Guggenheim–Anderson–DeBoer (GAB) sorption isotherm model. Measurements were performed in triplicate.

2.4.3. Kinetics of water absorption

The kinetics of water absorption was determined for all composites. Samples (rectangular strips of ~0.1 mm thickness) were first dried at 45 °C in an air-circulated oven over silica gel until constant weight. After weighing, they were conditioned at 25 °C in a desiccator containing saturated solution of KNO_3 to ensure a RH of 94%. Pullulan films are disintegrated very fast in contact with water. Because of this, the exposure at high moisture atmosphere, in order to study the kinetics of water uptake by the composites, was preferred instead of the classical technique of immersion in water (Anglès & Dufresne, 2000). The samples were removed at specific intervals and weighted. The water uptake of samples (WU) was calculated by Eq. (1), as follows:

$$WU(\%) = \frac{W_t - W_0}{W_0} \times 100 \quad (1)$$

where W_t and W_0 are the weights of the specimen at time t and the dry sample, respectively. At short times ($M_t/M_\infty \leqslant 0.6$) the mass of water absorbed at time t ($M_t = W_t - W_0$) can be expressed as:

$$\frac{M_t}{M_\infty} = \frac{2}{L}\left(\frac{D}{\pi}\right)^{1/2} t^{1/2} \quad (2)$$

where M_∞ is the mass of water absorbed at equilibrium, 2 L the thickness of film and D the diffusion coefficient. Plots of M_t/M_∞ as a function of $(t/L^2)^{1/2}$ were drawn for all composite films and for $M_t/M_\infty \leqslant 0.6$, and the diffusion coefficients were calculated from the slope of these plots. Differences in D values ($P < 0.05$) among samples were identified by analysis of variance using the Minitab Statistical Software, Release 13.1.

2.4.4. Water vapor permeability

Water vapor permeability (WVP) measurements of films were conducted at 25 °C using the ASTM (E96-63T) procedure modified for the vapor pressure at film underside according to McHugh, Avena-Bustillos, and Krochta (1993). Film discs, previously equilibrated at 53% RH for 48 h, were sealed to cups containing distilled water and the cups were placed in an air-circulated oven at 25 °C that was equilibrated at 53% RH using saturated solution of $MgCl_2 \times 6H_2O$. Film permeability was determined as described by Kristo, Biliaderis, and Zampraka (2006). The steady-state water vapor flow was reached within 2 h for all films. Slopes were calculated by linear regression and correlation coefficients for all reported data were >0.99. At least six replicates of each film type were tested for WVP. Differences in WVP ($P < 0.05$) among samples were identified by analysis of variance using the Minitab Statistical Software, Release 13.1.

2.4.5. Dynamic mechanical thermal analysis

Samples for DMTA analysis were thick specimens with dimensions of $0.5 \times 0.7 \times 0.15$ cm^3 that had been previously conditioned at various RH environments over saturated salt solutions for at least one month. The moisture content of each film was evaluated using the respective sorption isotherm. Before performing the DMTA analysis, the films were coated with silicon grease to avoid water evaporation. DMTA measurements were performed with a Mark III analyzer (Polymer Labs. Loughborough, UK) operated in the single cantilever bending mode (heating rate 2 °C min^{-1} and a strain level equal to a maximum displacement of 16 μm). The T_g was determined as the peak in tan δ at 3 Hz. DMTA thermal scans were also performed at five frequencies, i.e., 1, 3, 5, 10 and 20 Hz.

2.4.6. Large deformation tensile testing

Samples with starch filler content ranging from 0% to 40% (w/w) and conditioned at RH 53% for 10 days have been tested to evaluate the effect of nanofiller content in the large deformation mechanical properties of nanocomposites. Furthermore, the effect of sample moisture content on the mechanical properties of composites was studied using films containing 0%, 6%, 20% and 40% (w/w) starch nanocrystals after conditioning at 11%, 43%, 53% and 75% RH, for 10 days. Films were cut in dumbbell form specimens, their thickness was measured at three different points with a hand-held micrometer and an average value was obtained. The film thickness was around 80–90 μm. Samples were analyzed with a TA-XT2i instrument (Stable Micro systems, Godalming, Surrey, UK) in the tensile mode operated at ambient temperature and a crosshead speed of 60 mm min^{-1}. Young's modulus (E), maximum tensile strength (σ_{max}) and % elongation at break (% EB) were calculated from load-deformation curves of tensile measurements. Measurements represent an average of at least eight samples. The moisture content of samples, after storage, was determined by drying at 110 °C for 2 h.

3. Results and discussion

3.1. X-ray diffraction of materials

X-ray diffraction analyses have been performed on unfilled sample, composite films (filled with 6%, 15% and 30% w/w starch nanocrystals) as well as on powders of

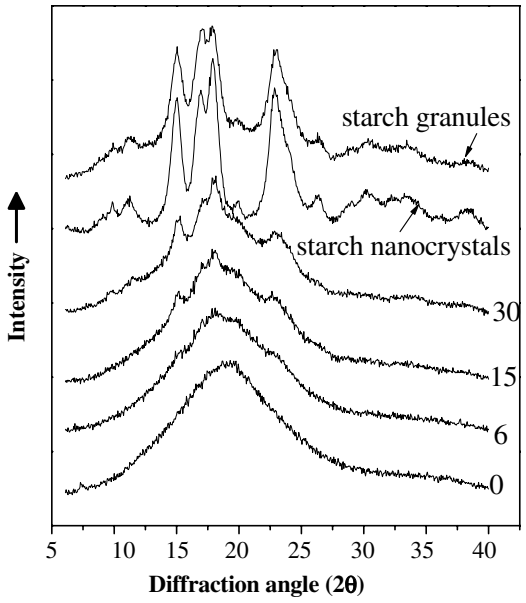

Fig. 1. X-ray diffraction patterns of native and acid-treated waxy maize starch granules as well as sorbitol-plasticized pullulan–starch nanocrystal composite films loaded with 0%, 6%, 15% and 30% (w/w) starch nanocrystals.

native waxy maize starch granules and air-dried starch crystals (Fig. 1). The waxy maize starch nanocrystals preserve the X-ray pattern of native waxy maize starch granules, typical of the A-type crystalline polymorph, and even showed sharper peaks than the native granules (Biliaderis et al., 1981). On the other hand, unfilled plasticized pullulan films are characterized by a broad hump centered on 19°, implying that the material is fully amorphous. When adding starch nanocrystals in the films, the typical diffraction peaks of crystals of A-type eventually appear. The magnitude of these peaks increases with the starch nanocrystal content of the film (Angellier et al., 2006).

3.2. Water sensitivity and moisture barrier properties of nanocomposites

3.2.1. Moisture sorption isotherms

The moisture sorption isotherms of sorbitol plasticized pullulan films containing different levels of starch nanocrystals are demonstrated in Fig. 2. The isotherms obtained were sigmoid in shape, showing a slow initial increase in moisture content with a_w increase up to 0.64 and a rapid increment in film water content with further augmentation of a_w. Such behavior is characteristic of materials rich in hydrophilic polymers and has extensively been reported in literature (e.g., Biliaderis et al., 1999; Cuq, Gontard, Aymard, & Guilbert, 1997; Diab, Biliaderis, Gerasopoulos, & Sfakiotakis, 2001; Hernández-Muñoz, Lagaron, Lopez-Rubio, & Gavara, 2004 etc.). As the concentration of filler increased, composite films absorbed less water, under similar a_w conditioning, and this difference was more pronounced at high moisture conditions ($a_w > 0.75$).

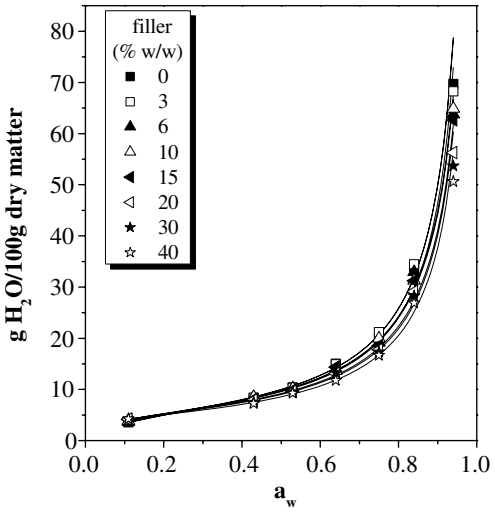

Fig. 2. Moisture sorption isotherms of sorbitol-plasticized pullulan–starch nanocrystal composite films filled with different nanofiller concentrations; solid lines represent the GAB model fit to the data.

The three parameter GAB model is the most generally accepted equation used to describe experimental water sorption data up to $a_w = 0.9$. The GAB equation is written as follows:

$$\frac{m}{m_m} = \frac{CKa_w}{(1 - Ka_w)[1 + (C - 1)Ka_w]}$$

Here, m_m represents the GAB monolayer value, and C is an indication of the strength of binding of water molecules to the sorption site, with greater C values denoting stronger bonds between the water molecule and the hydrophilic site. K is the ratio of the standard chemical potential of the indirectly bound water molecule and that of the molecule in the bulk liquid state. Values of K less than unity imply that the outermost hydration layer is formed by water molecules of lower activity than bulk water so that extra layers of water are required to be associated with the hydrated specimen before it can become fully accommodated into normal bulk water (Maggana & Pissis, 1999).

The GAB equation was fitted to the sorption data (solid lines in Fig. 2) and the calculated parameters are given in Table 1. As shown in Fig. 2, the predicted values of the GAB model corresponding to $a_w = 0.94$ are considerably higher than the experimental ones. The observed deviation is a consequence of unreliable accuracy of moisture determination at $a_w > 0.9$, because the values obtained are affected by osmotic, swelling and capillary phenomena (Biliaderis et al., 1999; Bizot, Le Bail, Leroux, Roger, & Buleon, 1997). The monolayer moisture (m_m) decreased and C increased with increasing the starch nanocrystals concentration in the film (Table 1), indicating that not only the hydrophilic sites of the polymeric matrix, but also starch nanoparticles serve as strong hydrophilic centers at which the first layer of water molecules is bonded with much higher binding intensity than the water of the indirectly bonded layer. The K values were similar for all the samples studied.

Table 1
Estimated parameters for water sorption data of sorbitol-plasticized pullulan–starch nanocrystal composite films using the GAB isotherm model at 25 °C

Starch nanocrystal content (% w/w)	m_m[a]	K[b]	C[b]	r^2
0	5.50	0.99	10.64	0.99
3	5.50	0.99	11.34	0.99
6	5.36	0.98	12.42	0.99
10	5.28	0.98	15.42	0.99
15	5.08	0.99	20.17	0.98
20	4.88	0.98	26.17	0.99
30	4.77	0.98	28.21	0.98
40	4.47	0.98	41.56	0.99

[a] m_m – monolayer value.
[b] K and C – GAB model parameters.

3.2.2. Kinetics of water absorption

The water uptake of samples conditioned at 94% RH, 25 °C was plotted as function of time (Fig. 3a). The two-stage water absorption pattern was obvious in all cases. At lower times ($t < 50$ h) the absorption kinetics is fast, whereas after that a slower absorption process follows, leading to a plateau. The water uptake for a given time is lower as the starch nanoparticle content is higher with the unfilled sample showing the highest degree of hydration. While the differences in water uptake of films with 6–15% (w/w) starch nanocrystal content were small, appreciable less water was absorbed by samples filled with high amounts of nanoparticles (20%, 30% and 40%, w/w). Thus, the water uptake values at equilibrium ranged between 69.7% and 50.6% (w/w) for unfilled samples and nanocomposites filled with 40% (w/w) starch nanocrystals, respectively (Fig. 3b). This result was in accordance with the findings reported above from moisture sorption isotherms. The diminution of the proportion of pullulan and sorbitol (considering the total dry matter of the sample) with the increment of starch nanocrystal content might have, at least partially, a contribution to the decrease of water sensitivity of the composite films, since pullulan adsorbs more water than starch crystallites, particularly at high water activities ($a_w > 0.8$) (Bizot et al., 1997). On the other hand, the phenomenon could be ascribed to the formation of a rigid three-dimensional starch nanocrystal network (due to the strong hydrogen bonding between the starch particles) that prevents the swelling of pullulan matrix (Dufresne & Vignon, 1998; Dufresne, Dupeyre, & Vignon, 2000), or to strong interactions between the filler and polymer chains, decreasing the swelling and water absorbance of the polymeric chains located in the interfacial regions (Gopalan Nair & Dufresne, 2003). Contradictory results are found in the literature about the effect of nanofillers on the equilibrium water uptake of nanocomposites. Results similar to the present study are presented by Anglès and Dufresne (2000), Dufresne and Vignon (1998) and Dufresne et al. (2000) in tunicin whiskers- or cellulose microfibrils-plasticized starch, by Lu, Weng, and Zhang (2004) in chitin whiskers reinforced soy protein isolate thermoplastics, by Lu, Weng, and Cao (2006), in ramie crystallites containing starch films, and by Sriupayo, Supaphol, Blackwell, and Rujiravanit (2005) in chitin whiskers–chitosan nanocomposite films. On the other hand, the incorporation of starch nanocrystals into latex (Dufresne & Cavaillé, 1998) or natural rubber (Angellier et al., 2005b) resulted in higher water uptake as the nanofiller content increased. The discrepancy could arise from the differences in compatibility between filler and matrix. The similar polar and hydrophilic character of matrix (biopolymers like starch or soy protein) and nanoparticles (tunicin or chitin whiskers, cellulose microfibrils, starch nanocrystals) leads probably to strong adhesion between the filler and matrix due to hydrogen bonding, which intensifies with increasing filler concentration, thus contributing to the evidenced lower water sensitivity of the highly hydrophilic composites. On the other hand, the poor interfacial compatibility of such hydrophilic particles with hydrophobic polymeric matrixes (e.g., latex, natural rubber) could result in a weak adhesion between filler and matrix and in low dispersion level of filler (Belgacem & Gandini, 2005). Furthermore, while these polymers have low affinity for water, the inclusion of polar and hydrophilic particles (which act

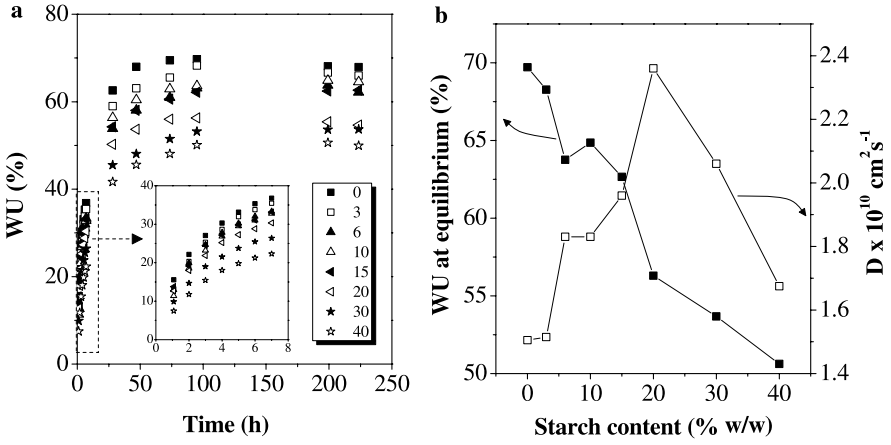

Fig. 3. (a) Kinetics of water absorption and (b) water uptake at equilibrium as well as the water diffusion coefficient values versus starch nanocrystal content, during conditioning at 94% RH of composites filled with different starch nanocrystal concentrations (ranging from 0% to 40%, w/w).

as strong hydrophilic centers that bound easily and strongly water) will probably bring about an increase in water uptake of the composites compared with the unfilled hydrophobic matrix.

As was shown in the experimental section, according to the Eq. (2), the slope of the plots of M_t/M_∞ as a function of $(t/L^2)^{1/2}$, drawn for $M_t/M_\infty \leqslant 0.6$, can be used to calculate the water diffusion coefficients (D). The evolution of D values for the studied samples conditioned at 94% RH as a function of nanofiller loading level is presented in Fig. 3b; in general, the calculated D values were within the range for other biopolymer nanocomposites such as soy protein–chitin whiskers (Lu et al., 2004), starch–ramie cellulose nanocrystallites (Lu et al., 2006) and starch–tunicin whiskers (Anglès & Dufresne, 2000). The D values increased to a maximum value of 2.36×10^{-10} cm^2 s^{-1} with a filler content up to 20% (w/w) nanocrystal and then decreased to 1.67×10^{-10} cm^2 s^{-1} for samples loaded with 40% (w/w) nanoparticles. The unfilled pullulan matrix showed the lower D value (1.5×10^{-10} cm^2 s^{-1}). Only the differences of the water diffusivities of the composite with 20% (w/w) nanostarch particles with that of unfilled samples as well as that of composites with 3% and 40% (w/w) filler content were statistically significant ($P < 0.05$). The higher water diffusivity of nanocomposites compared with the unfilled matrix in systems, where the polymer and filler are both very hydrophilic, is unusual in literature. Despite some increase in water D values at increased nanocrystal loading levels (with the D values of composites remaining always lower than those of unfilled counterparts) (Anglès & Dufresne, 2000; Mathew & Dufresne, 2002), the general trend reported in the literature for such systems is a decrease of water diffusivity as the filler content increases (Dufresne et al., 2000; Lu et al., 2004; Lu et al., 2006). In the present study, it seems that starch nanoparticles most likely form a continuous pathway to diffusion of water molecules through the composite where the filler content does not exceed 20% (w/w). At higher loading levels, the starch nanocrystals probably form a compact network structure, complicating the pathway of permeate and decreasing its diffusion through the composite system. However, finding answers on such a behavior is not an easy task, considering the complexity of a system consisting of four components, namely, pullulan, starch nanocrystals, sorbitol and water. The coexistence of different components in such heterogeneous systems could probably result in the formation of different regions (the region near the particle surface, the constrained polymer region that is directly affected by the filler and the unconstrained polymer region) with diverse properties and probably with different diffusion coefficients with respect to permeability characteristics (Beall, 2000).

3.2.3. Water vapor permeability

The WVP values of the studied films along with film thickness and RH estimates at the film underside are given in Table 2. The RH values at film underside were lower than the assumed 100% RH, due to the mass transfer resistance of stagnant air layer between the water surface and the film mounted in the cup, when the resistance to water transfer of highly hydrophilic film is small (McHugh et al., 1993). No significant differences ($P > 0.05$) were observed in WVP of unfilled samples and those containing up to 20% (w/w) nanocrystals. Adding starch nanofiller particles to the level of 30% and 40% (w/w) resulted in a significant ($P < 0.05$) decrease of WVP in a value lower than that of the unfilled system. It seems that the concentration of 20% (w/w) starch nanocrystals in composite films is a critical value for the WVP and water diffusivity. Above 20% (w/w) nanoparticle content a significant decrease in diffusion coefficient and the WVP of the composites was observed. The presence of such high filler concentrations, probably introduced a tortuous path for water molecule to pass through. The longer diffusive path that the penetrant molecules must travel, leads to the reduction of permeability (Sihna Ray & Okamoto, 2003).

Table 2
Effect of starch nanocrystal content on water vapor permeability (WVP) of sorbitol-plasticized pullulan–starch nanocrystal composite films

Starch nanocrystal content (% w/w)	Thickness (μm)	WVP (g s^{-1} m^{-1} Pa^{-1}) × 10^{10}	RH at film underside (%)
0	70	12.0[a*]	74
3	75	12.4[a]	74
6	70	12.5[a]	75
10	75	12.5[a]	75
15	72	12.8[a]	72
20	69	12.6[a]	75
30	73	9.6[b]	79
40	73	9.3[b]	79

[*] Different letters in the same column indicate significant differences ($P < 0.05$).

3.3. Thermo-mechanical properties of nanocomposites

3.3.1. Dynamic mechanical thermal analysis

The thermo-mechanical behavior of sorbitol-plasticized pullulan–starch nanocrystal composites was studied by dynamic mechanical thermal analysis (DMTA). The measurements were performed in thick specimens (~1.5 mm) loaded with 0%, 3%, 6%, 10% and 15% w/w starch nanocrystals. DMTA traces (log E' and tan δ vs. temperature at 3 Hz) of unfilled pullulan as well as composites loaded with 3% and 15% (w/w) of starch nanofiller and conditioned at 11% RH are shown in Fig. 4. The large drop of the elastic modulus and the intense peak of tan δ observed in the high temperature region correspond to the glass–rubber transition of pullulan. Usually, the position of the tanδ peak or the onset of E' drop is used as definition of glass transition temperature (T_g). As suggested by Fig. 4, the main tan δ peak (corresponding to the glass transition of pullulan) shifted to higher temperatures as starch nanocrystal content increased. Thus, the T_g (tan δ peak temperature) of unfilled pullulan matrix was 44 °C and increased to 57 and 76 °C for samples containing 3% and

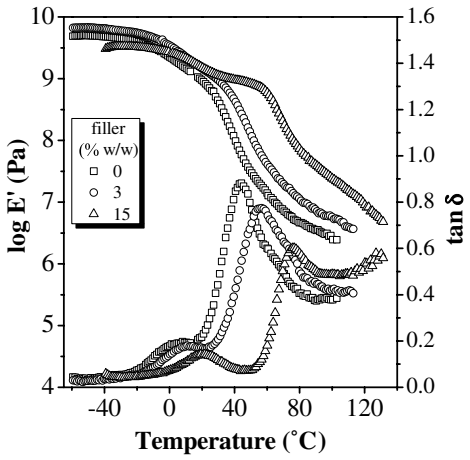

Fig. 4. DMTA plots (log E', tan δ) for sorbitol-plasticized pullulan–starch nanocrystal composite films containing 0%, 3% and 15% (w/w) filler particles conditioned at RH 11% (single cantilever bending mode, heating rate 2 °C min^{-1}, frequency 3 Hz).

15% (w/w) starch nanoparticles, respectively. These composite films had similar water content levels; 3.4% for unfilled pullulan and 3.5% and 4% for samples loaded with 3% and 15% (w/w) nanocrystals, respectively. Similarly, Lu et al. (2006), Angellier et al. (2006) and Avérous et al. (2001) reported a significant increase of T_g of plasticized starch matrix with increasing concentration of ramie, starch nanocrystals and cellulose fibers, respectively. As the shift of the main relaxation to higher temperatures usually indicates restricted molecular movement, these authors attributed the observed increase in T_g to the strong interactions through hydrogen bonding between the amorphous polymeric matrix and the reinforcing particles. Such an interfacial H-bonding leads to a strong absorption of polymer chains on the surface of nanoparticles (Smith et al., 2003) and formation of 'trapped entanglements' of the polymer segments, resulting in the obstruction of mobility not only of polymer chains attached to the particle surface, but also those having no direct contact with the filler surfaces. As the filler concentration increases, the boundary layers of polymer–nanoparticles begin to overlap due to the smaller distance between particles (Zhu & Sternstein, 2003). The existence of such an interphase of immobilized matrix in contact with the particle surface (Chazeau et al., 1999) that probably has a higher T_g than the rest of the matrix, brings about the noticed increase of T_g as a function of composite filler concentration (Anglès & Dufresne, 2000; Theocaris & Spathis, 1982; Wetzel, Haupert, & Zhang, 2003). Molecular simulations have shown the slowing down of the dynamics of the polymer chains near the confining surface of a particle (Dionne et al., 2005; Smith, Vladkov, & Barrat, 2005), thus supporting the concept of immobilized matrix interphase. However, other investigators found no significant changes of the temperature position of the main relaxation upon nanofiller addition (Anglès & Dufresne, 2001; Chazeau et al., 1999; Dufresne et al., 1996; Dubief et al., 1999; Favier et al., 1995b; Morin & Dufresne, 2002). Theocaris and Spathis (1982), based on the concept of interphase suggested that the glass transition of the composite material is determined by the combination of the glass transitions of interphase and matrix. Thus, if the T_g of interphase is greater than the T_g of the matrix, the composite shows a T_g higher than that of the matrix and vice versa.

The magnitudes of tan δ peak and of the storage modulus drop were reduced with increasing amounts of starch filler particles loaded in the pullulan matrix. The decrease in the magnitude of tanδ peak was related to a possible decrease of flexibility of the polymer chains through the strong polymer filler interaction as was evidenced above, and/or to the decrease of the amount of the relaxing phase since, the increment of filler content in the composite leads to the diminution of the proportion of the pullulan in the sample (Angellier et al., 2006). At rubbery state, composites showed higher storage modulus E' values than the unfilled samples and the E' increased with filler content (Fig. 4). For example, the storage modulus of composite films containing 3% and 15% (w/w) nanocrystals (around 5.3 and 22.9 MPa at 100 °C, respectively) is about 2 and 9 times higher, respectively, than that of the unfilled matrix (around 2.6 MPa at 100 °C). This reinforcing effect was low compared to experimental data reported by Angellier, Molina-Boisseau, and Dufresne (2005a) for starch nanocrystal filled natural rubber (e.g., E' of composite with 10% (w/w) nanocrystals was 10 times higher than that of the unfilled matrix), but was similar to that of poly(styrene-co-butyl acrylate) filled with 10% (w/w) starch nanocrystals (Angellier, Putaux, Molina-Boisseau, Dupeyre, & Dufresne, 2005c).

In all samples, a relaxation tan δ peak was observed at temperatures lower than that of the α-relaxation (Figs. 4 and 5a and b). The properties of this relaxation in pullulan films plasticized with different levels of sorbitol were described in a previous investigation (Kristo & Biliaderis, 2006). It was shown that the temperature of this low temperature (low-T) transition corresponded to the region of the T_g of sorbitol, but was somewhat higher than the T_g of sorbitol (at the respective water content), suggesting that it most likely reflects the relaxation of a sorbitol-rich phase whose T_g increases by the presence of the polymer domains (Moates, Noel, Parker, & Ring, 2001) due to an increase in the average molecular weight (Cherian, Gennadios, Weller, & Chinachoti, 1995). Here, for samples conditioned at 11% RH, the position of low-T transition was shifted at higher temperatures with increasing the concentration of starch nanocrystals in the composite, as shown in Fig. 4. Thus, the low-T transition was observed at 7.8 °C for unfilled samples, but moved to 12 and 20 °C when 3% and 15% (w/w) nanofiller was added, respectively. It seems that the presence of nanoparticles influenced the relaxation of the sorbitol-rich phase either by slowing down the molecular mobility of sorbitol or by movement restriction of polymer chains present in the sorbitol-rich phase. However, Angellier et al. (2006) observed no shift on the temperature

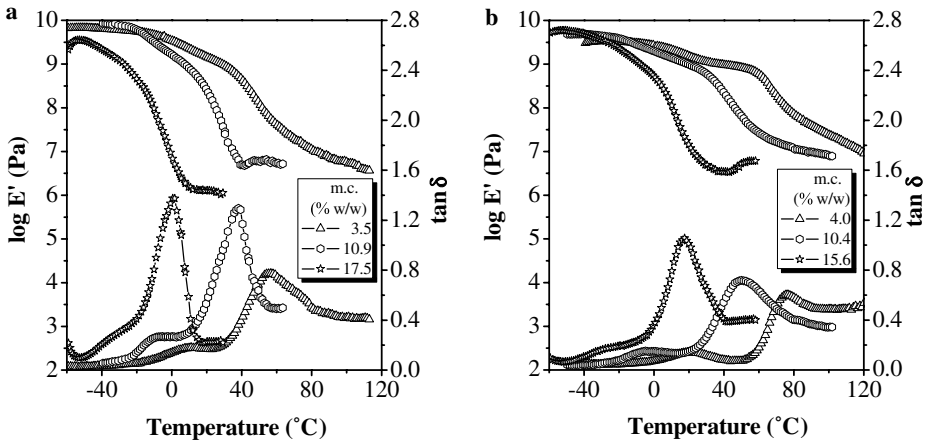

Fig. 5. DMTA plots (log E', tan δ) for sorbitol-plasticized pullulan–starch nanocrystal composite films loaded with (a) 3% and (b) 15% (w/w) starch nanofillers at different hydration levels (single cantilever bending mode, heating rate 2 °C min^{-1}, frequency 3 Hz).

position of the low-T relaxation (corresponding to the α-relaxation of glycerol used as plasticizer) when the starch nanocrystal content increased to 15% (w/w).

In Figs. 5a and b the effect of moisture content on the evolution of thermo-mechanical properties of composites filled with 3% and 15% (w/w) starch nanocrystals, respectively, is depicted. As the water content of the nanocomposites increased, both low-T and main relaxation shifted to lower temperatures, a behavior ascribed to the well-known plasticizing action of water. Also, the low-T tan δ peak tends to converge with the α-relaxation peak in samples with high water content (>15%). This merging of both relaxations has been previously described (Kristo & Biliaderis, 2006; Lourdin, Ring, & Colonna, 1998). The decrease of the main tan δ peak intensity with increasing nanofiller content described above, was observed in samples conditioned at 53% and 75% RH (m.c. 10.5–10.9% and 15.6–17.5%, respectively) as well.

As was evidenced above for samples conditioned at low RH (11%), the T_g and low-T transition temperature of the composite materials increased with starch nanocrystal content. In addition, a similar trend was observed with the T_g of nanocomposites conditioned at more humid environments (53% and 75% RH), but the difference in T_g of filled samples compared to the unfilled ones declined with increasing sample hydration (Fig. 6a). On the other hand, the temperature position of the low-T relaxation remained independent of nanofiller content when samples were conditioned at 53% and 75% RH, as shown in Fig. 6b. At low levels of hydration (m.c. 3.5–4% w/w), water molecules strongly interact through hydrogen bonding with the hydroxyl groups of pullulan, sorbitol and/or starch crystals and most likely assist in enhancing the immobilization (introduced by starch nanocrystals) of the pullulan chains or sorbitol amorphous domains. This led both transitions assigned to the main relaxation of pullulan and sorbitol to shift towards much higher temperatures compared with the unfilled sample. At higher water contents, the formation of water–water bridges caused the loosening of this H-bond network and the weakening of matrix–particle and/or particle–particle interactions leading consequently, to higher mobility of the pullulan–particles interphase.

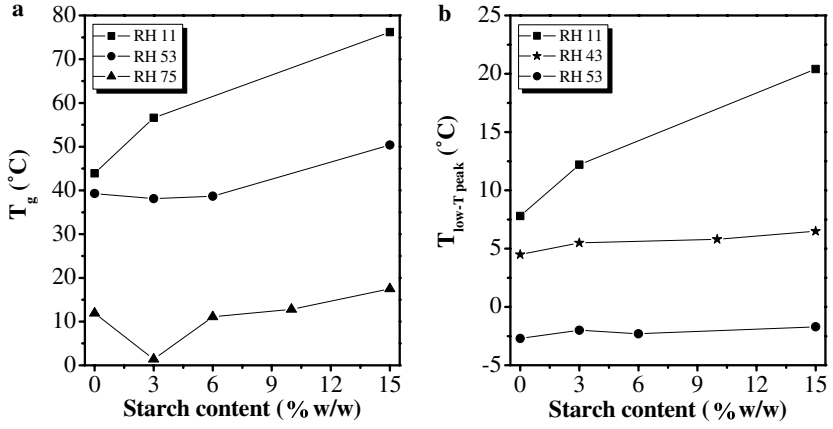

Fig. 6. Effect of starch nanocrystal content and humidity conditioning at (a) glass transition temperature (T_g) of α-relaxation and (b) temperature of transition observed at low temperature; both temperatures were determined from the temperature position of the respective tan δ peaks (3 Hz).

However, the degree of attenuation of interactions between polymer and particles was not high enough to prevent the T_g augmentation of composites as a function of nanoparticle content. Concerning the low-T transition, the plasticizing action of water was able to cancel the probable slowing down of mobility of sorbitol or polymer domains in the sorbitol-rich phase of composites (caused by interaction with filler particles) and to maintain the temperature of low-T transition at the same level as that of unfilled system.

DMTA thermal scans at five frequencies were performed for unfilled sample and composites containing 3, 6 and 10 wt% starch nanocrystals at two different levels of moisture content. Since both α-relaxation and low-T transition are thermally activated processes, the tanδ peaks of α-relaxation and low-T transition shifted to higher temperatures with increasing frequency. The apparent activation energies for both relaxations were determined from the Arrhenius relationship:

$$\ln\frac{f}{f_o} = -\frac{E_a}{RT}$$

Table 3
Apparent activation energy (E_a) of the α- and the low temperature (low-T) relaxations estimated for sorbitol-plasticized pullulan–starch nanocrystal composite films at different moisture content

Starch nanocrystal content (% w/w)	E_a (kJ/mol)		
	m. c. (% w/w)	α-relaxation	Low-T relaxation
0	5.1	283.5 (0.98)[a]	174.6 (0.98)
	18.2	163.0 (0.99)	–
3	6.0	291.3 (0.96)	164.7 (0.99)
	17.7	226.5 (0.98)	–
6	–	–	–
	16.9	255.9 (0.99)	–
10	7.5	334.4 (0.99)	171.1 (0.99)
	17.9	229.6 (0.98)	–

[a] Numbers in parenthesis are the regression coefficients (r^2) of the respective Arrhenius plots $\ln(f/f_0) = -E_a/RT$.

The calculated apparent activation energies (E_a) along with the regression coefficients of the Arrhenius plots for all samples containing different moisture levels are summarized in Table 3. The high E_a values of the nanocomposite samples, varying between 163 and 334 kJ/mol for the α-relaxation process and between 165 and 175 kJ/mol for low-T transition are typical of main relaxations associated with the glass–rubber transition and here, corresponded to the α-relaxation of pullulan and sorbitol, respectively. Thus, the E_a values corresponding to α-relaxation of polymers are generally reported to be in the range 200–400 kJ/mol (Kalichevsky, Blanshard, & Marsh, 1993; Champion, Le Meste, & Simatos, 2000). The apparent E_a values of both transitions for nanocomposite films were close to those of the unfilled sample at similar water content and did not show any dependence on the filler content, what is in accordance with the finding of Anglès and Dufresne (2001) for starch/tunicin whiskers nanocomposites. The E_a values of the primary relaxation generally reduced with increasing hydration level of samples that is in good agreement with previous findings of Lazaridou and Biliaderis (2002), Lazaridou, Biliaderis, and Kontogiorgos (2003), Elicegui, del Val, Bellenger, and Verdu (1997) and Kristo and Biliaderis (2006).

3.3.2. Large deformation mechanical testing

The mechanical behavior of sorbitol plasticized pullulan films filled with various levels (0–40%, w/w) of starch nanocrystals and conditioned at 53% RH was investigated by large deformation tensile tests at room temperature. The moisture content of all samples after conditioning for 10 days at RH 53% was between 8.3% and 9.1% (w/w).

Fig. 7a shows the evolution of Young modulus (E) and maximum tensile strength (σ_{max}) of reinforced composites as function of filler level, whereas the inset plot in Fig. 7a presents the progress of the relative Young modulus ($E_R = E$ composite/E matrix) and relative strength

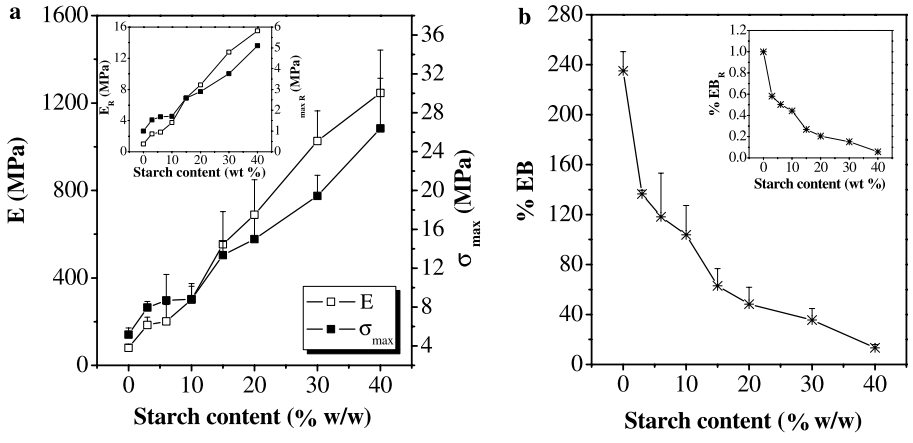

Fig. 7. Effect of starch nanocrystal concentration on (a) tensile modulus (E) and tensile strength (σ_{max}) and (b) % elongation at break (% EB) as determined from tensile tests of sorbitol-plasticized pullulan–starch nanocrystal composite films following conditioning at 53% RH (the moisture content of all samples was within 8.3% and 9.1% w/w); insets show (a) the relative tensile modulus ($E_R = E$ composite/E matrix) and the relative strength ($\sigma_{maxR} = \sigma_{max}$ composite/σ_{max} matrix) and (b) the relative % elongation at break (% EB_R = % $EB_{composite}$/ % EB_{matrix}) versus starch nanoparticle content.

($\sigma_{maxR} = \sigma_{max}$ composite/σ_{max} matrix) as a function of nanoparticle content. The systematic and significant increase of both parameters with starch nanofiller content increase pointed out the great reinforcing effect of starch nanocrystal addition on plasticized pullulan films. Thus, E and σ_{max} of composites filled with 40% (w/w) starch nanocrystals increased ~16 and 5 times compared with E and σ_{max} of the unfilled system, respectively. Such a reinforcing effect was observed in waxy maize starch nanocrystal filled thermoplastic starch (Angellier et al., 2006), in cellulose fiber reinforced thermoplastic starch or silk fibroin (Avérous, Fringant, & Moro, 2001; Noshiki et al., 2002) and in polypropylene composites loaded with residual softwood fibers (Anglès et al., 1999). Moreover, the reinforcement rate was higher when filler loading was more than 10% (w/w) as compared with nanoparticle content up to 10% (w/w). Similarly, Angellier et al. (2006) reported higher reinforcement effect on E and σ_{max} of starch composites when waxy maize starch nanocrystals exceeded 10% (w/w).

Owing to the very high specific surface area provided by nanoparticles, the filler–matrix interfacial interactions play a key role in the mechanical properties of nanocomposites (Wetzel et al., 2003). Well distributed particles with an adequate interfacial bonding between filler and matrix allows the effective transfer of stress through a shear mechanism from the matrix to the particles that can efficiently carry the load and enhance the strength of the composite (Abdelmouleh, Boufi, Belgacem, Dufresne, & Gandini, 2005; Ahmed & Jones, 1990; Anglès et al., 1999; Brown & Ellyin, 2005; Sihna Ray & Okamoto, 2003; Wetzel et al., 2003). Hence, the increase in modulus and strength, as observed here for pullulan–starch nanocomposites show the efficient stress transfer via the interface, further demonstrating the strong interfacial bonding between pullulan matrix and starch nanocrystals as was also assumed from the DMTA measurements. The evidenced improvement of mechanical properties of nanocomposites under nonlinear deformation has been related to the ability of nanoparticles to induce additional failure and energy consuming mechanisms such as matrix shear deformation, particle debonding, crack front pinning and crack deviation. Nanosized particles can deviate or pin the crack front bringing about a higher energy absorption in the composite (Ahmed & Jones, 1990; Wetzel et al., 2003).

Fig. 7b shows the dependence of % elongation at break (%EB) on the filler content whereas the inset plot shows the relative % EB (% EB_R = % $EB_{composite}$/% EB_{matrix}) as function of starch nanofiller concentration. The unfilled sample displayed a ductile behavior at room temperature, with EB ~235%. The addition of only 3% of starch particles resulted in a significant diminution of % EB to 136% (% $EB_R = 0.6$). A further increase in the filler content brought about the gradual decrease of % EB up to 13% for 40% nanocrystal addition (% $EB_R = 0.06$). The decrease in EB with the rigid filler addition is a well-known phenomenon (Angellier et al., 2006; Anglès et al., 1999; Avérous et al., 2001) that is related to the differences in the rigidity between matrix and fillers. Because of the rigid nature of the fillers, most of the system deformation under high strain comes from the polymer. Consequently, the actual deformation experienced only by the polymeric matrix is much greater than the measured deformation of the sample. Thus, the polymer reaches the failure strain limit at a

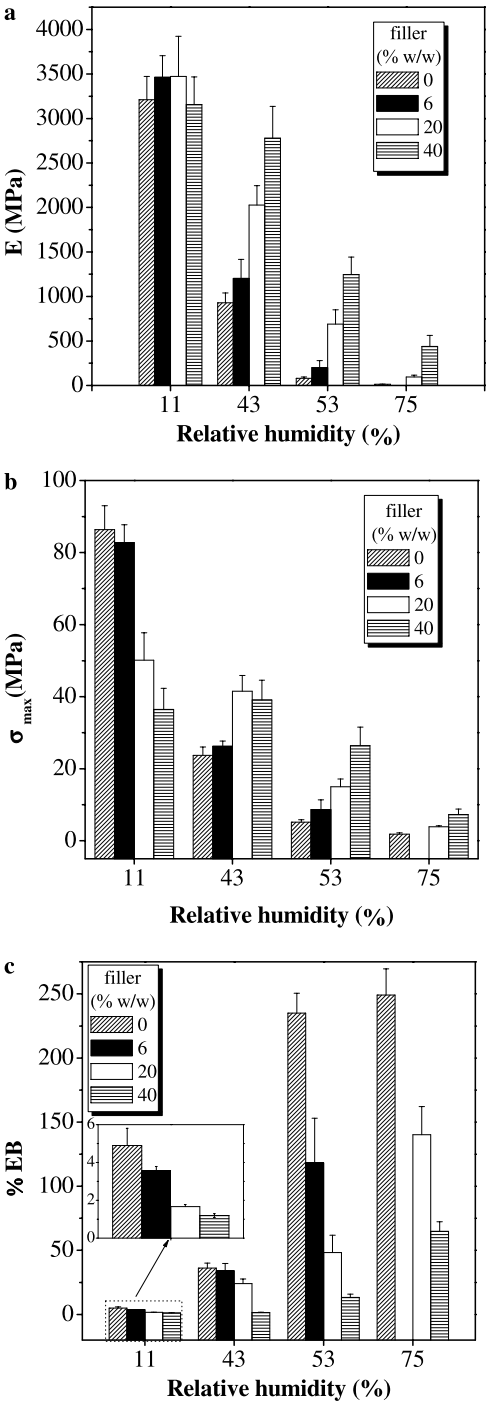

Fig. 8. Effect of conditioning at different moisture environments on (a) tensile modulus (E), (b) tensile strength (σ_{max}) and (c) % elongation at break (% EB) as determined from tensile tests of sorbitol-plasticized pullulan–starch nanocrystal composite films containing 0%, 6%, 20% and 40% (w/w) nanofiller particles.

Table 4
Relative mechanical properties of sorbitol-plasticized pullulan–starch nanocrystal composite films filled with 0%, 6%, 20% and 40% (w/w) starch nanocrystals after conditioning at different RH environments

RH	Starch nanocrystal content (% w/w)	E_R [a] $= E_{composite}/E_{matrix}$	σ_{maxR} [b] $= \sigma_{max\,composite}/\sigma_{max\,matrix}$	% EB_R [c] = % $EB_{composite}$/% EB_{matrix}
11	0	1.00	1.00	1.00
	6	1.08	0.96	0.73
	20	1.08	0.58	0.34
	40	0.98	0.42	0.24
43	0	1.00	1.00	1.00
	6	1.30	1.11	0.94
	20	2.18	1.75	0.66
	40	2.99	1.65	0.04
53	0	1.00	1.00	1.00
	6	2.51	1.68	0.50
	20	8.58	2.90	0.21
	40	15.52	5.10	0.06
75	0	1.00	1.00	1.00
	20	7.74	2.12	0.56
	40	35.46	4.01	0.26

[a] Relative tensile modulus.
[b] Relative maximum tensile strength.
[c] Relative % elongation at break.

lower total deformation (Anglès et al., 1999; Wetzel et al., 2003).

Due to the great susceptibility to water of materials that consist of highly hydrophilic components such as polysaccharides, it is relevant to study the properties of such systems at different hydration levels. To investigate the effect of water content on the observed reinforcement of pullulan–starch nanocrystal composites, unfilled samples as well as composites with nanofiller loading of 6%, 20% and 40% (w/w) were conditioned for 10 days at 11%, 43%, 53% and 75% RH. The mechanical properties of samples represented by E, σ_{max} and % EB, as function of RH conditioning and nanofiller level are depicted in Figs. 8a–c. The classic plasticizing effect of water was quite obvious in all cases, independently of the nanocrystal content. Significant decrease of E and σ_{max} and increase of % EB ($P < 0.05$) was observed as RH increased from 11% to 75%. It was of further interest to examine more closely if the reinforcement pattern described above in the nanocomposites stored at 53% RH is also followed under varying moisture conditions. As indicated by Figs. 8a–c, the increase in E and σ_{max} and the decline of % EB with filler content was evident not only at 53% RH, but also following conditioning at 43% and 75% RH. The reinforcing effect was greater at high filler contents (20% and 40% w/w). The comparison of relative mechanical properties of composites at different RH conditions gives a further opportunity to evaluate the behavior of composites as function of sample hydration level. The relative parameters E_R, σ_{maxR} and % EB_R are defined as the ratio of the value of the respective property of nanocomposite to the one of the unfilled matrix at specific water content, as was described above. As shown in Table 4, the relative reinforcing effect of waxy maize starch nanocrystals was more significant when the water content was high. Thus, the E values of pullulan–starch nanocomposites reinforced with 40% (w/w) starch nanocrystals was 3, 15 and 35 times higher than that of unfilled system conditioned at 43%, 53% and 75% RH, respectively. Also, the decrease of the % EB caused by incorporation of filler, is lower at 75% RH than at 43% and 53% RH. Angellier et al. (2006) reported more pronounced reinforcing effects of waxy maize starch nanocrystals incorporated in thermoplastic starch matrixes and a lower decrease of the strain at break in the case of highly plasticized systems. A different behaviour was observed when films were conditioned at low moisture conditions (11% RH). As shown in Figs. 8a and b, samples conditioned at 11% RH resulted in non-significant ($P > 0.05$) changes of E and in a significant decrease ($P < 0.05$) of σ_{max} as function of filler loading level. For the last parameter, the decrease was more important at high filler contents. The reduction of composite strength is not unexpected even in nanocomposite systems (Brown & Ellyin, 2005). This is explained by an increased tendency for aggregation that accompanies the increased surface area of such small particles. Particularly, at high filler contents, where more agglomerates are likely to be formed, they could serve as stress concentrators locally, easily inducing the initiation of final failure (Brown & Ellyin, 2005; Wetzel et al., 2003).

4. Conclusions

Sorbitol-plasticized pullulan films filled with waxy maize starch nanocrystals showed substantially altered mechanical and water resistance properties compared with the unfilled system. Lower water uptake at equilibrium was noticed particularly at high filler loading levels. Furthermore, enhanced water barrier properties were exhibited by composites containing >20% (w/w) nanoparticles. The T_g related to the α-relaxation of pullulan shifted to higher temperatures as the amount of nanofiller increased. This trend was independent of the sample hydration level.

A drastic increase of the Young modulus and the maximum tensile strength as well as a significant diminution of the percentage of elongation at break with the nanofiller content was observed after sample conditioning at diverse RH environments (from 43% to 75%). These findings supported the crucial role of strong interfacial bonding between starch nanofiller and pullulan matrix. The relative reinforcing effect of starch nanocrystals was more significant at high hydration levels.

Acknowledgements

E. Kristo thank the State Scholarship Foundation (IKY) of Greece for awarding her a graduate fellowship. The authors also wish to acknowledge the assistance of Dr. N. Barbayiannis (Laboratory of Soil Chemistry) for conducting the X-ray diffraction measurements.

References

Abdelmouleh, M., Boufi, S., Belgacem, M. N., Dufresne, A., & Gandini, A. (2005). Modification of cellulose fibers with functionalised silanes: effect of the fiber treatment on the mechanical performances of cellulose-thermoset composites. *Journal of Applied Polymer Science, 98*, 974–984.

Ahmed, S., & Jones, F. R. (1990). A review of particulate reinforcement theories for polymer composites. *Journal of Materials Science, 25*, 4933–4942.

Angellier, H., Molina-Boisseau, S., Dole, P., & Dufresne, A. (2006). Thermoplastic starch–waxy maize starch nanocrystals nanocomposites. *Macromolecules, 7*, 531–539.

Angellier, H., Molina-Boisseau, S., & Dufresne, A. (2005a). Mechanical properties of waxy maize starch nanocrystal reinforced natural rubber. *Macromolecules, 38*, 9161–9170.

Angellier, H., Molina-Boisseau, S., Lebrun, L., & Dufresne, A. (2005b). Processing and structural properties of waxy maize starch nanocrystals reinforced natural rubber. *Macromolecules, 38*, 3783–3792.

Angellier, H., Putaux, J. L., Molina-Boisseau, S., Dupeyre, D., & Dufresne, A. (2005c). Starch nanocrystal fillers in an acrylic polymer matrix. *Macromolecular Symposium, 221*, 95–104.

Anglès, M. N., & Dufresne, A. (2000). Plasticized starch/tunicin whiskers nanocomposites. 1. Structural analysis. *Macromolecules, 33*, 8344–8353.

Anglès, M. N., & Dufresne, A. (2001). Plasticized starch/tunicin whiskers nanocomposites. 2. Mechanical behavior. *Macromolecules, 34*, 2921–2931.

Anglès, M. N., Salvadó, J., & Dufresne, A. (1999). Steam-exploded residual softwood-filled polypropylene composites. *Journal of Applied Polymer Science, 74*, 1962–1977.

Avérous, L., Fringant, C., & Moro, L. (2001). Plasticized starch–cellulose interactions in polysaccharide composites. *Polymer, 42*, 6565–6572.

Azizi Samir, M. A. S., Alloin, F., & Dufresne, A. (2005). Review of resent research into cellulose whiskers, their properties and their application in the nanocomposite field. *Biomacromolecules, 6*, 612–626.

Beall, G. W. (2000). New conceptual model for interpreting nanocomposite behavior. In T. J. Pinnavaia & G. W. Beall (Eds.), *Polymer–clay nanocomposites* (pp. 267–280). Chichester: John Wiley & Sons, Ltd.

Belgacem, M. N., & Gandini, A. (2005). The surface modification of cellulose fibres for use as reinforcing elements in composite materials. *Composite Interfaces, 12*, 41–75.

Biliaderis, C. G., Grant, D. R., & Vose, J. R. (1981). Structural characterization of legume starches. II. Studies on acid-treated starches. *Cereal Chemistry, 8*, 502–507.

Biliaderis, C. G., Lazaridou, A., & Arvanitoyannis, I. (1999). Glass transition and physical properties of polyol-plasticized pullulan–starch blends at low moisture. *Carbohydrate Polymers, 40*, 29–47.

Bizot, H., Le Bail, P., Leroux, B., Roger, P., & Buleon, A. (1997). Calorimetric evaluation of the glass transition in hydrated, linear and branched polyanhydroglucose compounds. *Carbohydrate Polymers, 40*, 33–50.

Brown, G. M., & Ellyin, F. (2005). Assessing the predictive capability of two-phase models for the mechanical behavior of alumina/epoxy nanocomposites. *Journal of Applied Polymer Science, 98*, 869–879.

Champion, D., Le Meste, M., & Simatos, D. (2000). Towards an improved understanding of glass transition and relaxations in foods: molecular mobility in the glass transition range. *Trends in Food Science and Technology, 11*, 41–55.

Chazeau, L., Cavaillé, J. Y., Canova, G., Dendievel, R., & Boutherin, B. (1999). Viscoelastic properties of plasticized PVC reinforced with cellulose whiskers. *Journal of Applied Polymer Science, 71*, 1797–1808.

Cherian, G., Gennadios, A., Weller, C., & Chinachoti, P. (1995). Thermomechanical behaviour of wheat gluten films: effect of sucrose, glycerin and sorbitol. *Cereal Chemistry, 72*, 1–6.

Cuq, B., Gontard, N., Aymard, C., & Guilbert, S. (1997). Relative humidity and temperature effects on mechanical and water vapor barrier properties of myofibrillar protein-based films. *Polymer Gels and Networks, 5*, 1–15.

Diab, T., Biliaderis, C. G., Gerasopoulos, D., & Sfakiotakis, E. (2001). Physico-chemical properties and application of pullulan edible films and coatings in fruit preservation. *Journal of Science of Food and Agriculture, 81*, 988–1000.

Dionne, P. J., Ozisik, R., & Picu, C. R. (2005). Structure and dynamics of polyethylene nanocomposites. *Macromolecules, 38*, 9351–9358.

Dubief, D., Samain, E., & Dufresne, A. (1999). Polysaccharide microcrystals reinforced amorphous poly(β-hydroxyoctanoate) nanocomposite materials. *Macromolecules, 32*, 5765–5771.

Dufresne, A., & Cavaillé, J. Y. (1998). Clustering and percolation effects in micrcrystalline starch-reinforced thermoplastic. *Journal of Polymer Science: Part B: Polymer Physics, 36*, 2211–2224.

Dufresne, A., Cavaillé, J. Y., & Helbert, W. (1996). New nanocomposite materials: microcrystalline starch reinforced thermoplastic. *Macromolecules, 29*, 7624–7626.

Dufresne, A., Dupeyre, D., & Vignon, M. R. (2000). Cellulose microfibrils from potato tuber cells: processing and characterization of starch–cellulose microfibril composites. *Journal of Applied Polymer Science, 76*, 2080–2092.

Dufresne, A., Kellerhals, M. B., & Witholt, B. (1999). Transcrystallization in Mcl-PHAs/cellulose whiskers composites. *Macromolecules, 32*, 7396–7401.

Dufresne, A., & Vignon, M. R. (1998). Improvement of starch film performances using cellulose microfibrils. *Macromolecules, 31*, 2693–2696.

Elicegui, A., del Val, J. J., Bellenger, V., & Verdu, J. (1997). A study of plasticization effects in poly(vinyl chloride). *Polymer, 38*, 1647–1657.

Favier, V., Canova, G. R., Cavaillé, J. Y., Chanzy, H., Dufresne, A., & Gauthier, C. (1995b). Nanocomposites materials from latex and cellulose whiskers. *Polymers for Advanced Technologies, 6*, 351–355.

Favier, V., Chanzy, H., & Cavaillé, J. Y. (1995a). Polymer nanocomposites reinforced by cellulose whiskers. *Macromolecules, 28*, 6365–6367.

Gidley, M. J., Cooke, D., & Ward-Smith, S. (1993). Low moisture polysaccharide systems: thermal and spectroscopic aspects. In J. M. V. Blanshard & P. J. Lillford (Eds.), *The glassy state in foods* (pp. 303–316). Nottingham: University Press.

Gopalan Nair, K., & Dufresne, A. (2003). Crab shells chitin whiskers reinforced natural rubber nanocomposites. 1. Processing and swelling behavior. *Biomacromolecules, 4*, 657–665.

Hernández-Muñoz, P., Lagaron, J. M., Lopez-Rubio, A., & Gavara, R. (2004). Gliadins polymerized with cysteine: effects on the physical and water barrier properties of derived films. *Biomacromolecules, 5*, 1503–1510.

Kalichevsky, M. T., Blanshard, J. M. V., & Marsh, R. D. L. (1993). Applications of mechanical spectroscopy to the study of glassy biopolymers and related systems. In J. M. V. Blanshard & P. J. Lillford (Eds.), *The glassy state in foods* (pp. 133–156). Nottingham: University Press.

Kristo, E., & Biliaderis, C. G. (2006). Water sorption and thermomechanical properties of water/sorbitol-plasticized composite biopolymer films: caseinate–pullulan bilayers and blends. *Food Hydrocolloids, 20*, 1057–1071.

Kristo, E., Biliaderis, C. G., & Zampraka, A. (2006). Water vapor barrier and tensile properties of composite caseinate–pullulan films: biopolymer composition effects and impact of beeswax lamination. *Food chemistry,* in press.

Lazaridou, A., & Biliaderis, C. G. (2002). Thermophysical properties of chitosan, chitosan–starch and chitosan–pullulan films near the glass transition. *Carbohydrate Polymers, 48*, 179–190.

Lazaridou, A., Biliaderis, C. G., & Kontogiorgos, V. (2003). Molecular weight effects on solution rheology of pullulan and mechanical properties of its films. *Carbohydrate Polymers, 52*, 151–166.

Lourdin, D., Ring, S. G., & Colonna, P. (1998). Study of plasticizer–oligomer and plasticizer–polymer interactions by dielectric analysis: maltose–glycerol and amylose–glycerol–water systems. *Carbohydrate Research, 306*, 551–558.

Lu, Y., Weng, L., & Cao, X. (2006). Morphological, thermal and mechanical properties of ramie crystallites-reinforced plasticized starch biocomposites. *Carbohydrate Polymers, 63*, 198–204.

Lu, Y., Weng, L., & Zhang, L. (2004). Morphology and properties of soy protein isolate thermoplastics reinforced with chitin whiskers. *Biomacromolecules, 5*, 1046–1051.

Maggana, C., & Pissis, P. (1999). Water sorption and diffusion studies in an epoxy resin system. *Journal of Polymer Science: Part B: Polymer Physics, 37*, 1165–1182.

Mathew, A. P., & Dufresne, A. (2002). Morphological investigation of nanocomposites from sorbitol plasticized starch and tunicin whiskers. *Biomacromolecules, 3*, 609–617.

McHugh, T. H., Avena-Bustillos, R., & Krochta, J. M. (1993). Hydrophilic edible films: modified procedure for water vapor permeability and explanation of thickness effects. *Journal of Food Science, 58*, 899–903.

Moates, G. K., Noel, T. R., Parker, R., & Ring, S. G. (2001). Dynamic mechanical and dielectric characterization of amylose–glycerol film. *Carbohydrate Polymer, 44*, 247–253.

Morin, A., & Dufresne, A. (2002). Nanocomposites of chitin whiskers from riftia tubes and poly(caprolactone). *Macromolecules, 35*, 2190–2199.

Noshiki, Y., Nishiyama, Y., Wada, M., Kuga, S., & Magoshi, J. (2002). Mechanical properties of silk fibroin–microcrystalline cellulose composite films. *Journal of Applied Polymer Science, 86*, 3425–3429.

Putaux, J. L., Molina-Boisseau, S., Momaur, T., & Dufresne, A. (2003). Platelet nanocrystals resulting from the disruption of waxy maize starch granules by acid hydrolysis. *Biomacromolecules, 4*, 1198–1202.

Robin, J. P., Mercier, C., Charbonnière, R., & Guilbot, A. (1974). Lintnerized starches. Gel filtration and enzymatic studies of insoluble residue from prolonged acid treatment of potato starch. *Cereal Chemistry, 51*, 389–406.

Sihna Ray, S., & Okamoto, M. (2003). Polymer/layered silicate nanocomposites: a review from preparation to processing. *Progress in Polymer Science, 28*, 1539–1641.

Smith, J. S., Bedrov, D., & Smith, G. D. (2003). A molecular dynamics simulation study of nanoparticle interactions in a model polymer–nanoparticle composite. *Composite Science and Technology, 63*, 1599–1605.

Smith, K. A., Vladkov, M., & Barrat, J. L. (2005). Polymer melt near a solid surface: a molecular dynamics study of chain conformations and desorption dynamics. *Macromolecules, 38*, 571–580.

Sriupayo, J., Supaphol, P., Blackwell, J., & Rujiravanit, R. (2005). Preparation and characterization of α-chitin whisker-reinforced chitosan nanocomposite films with or without heat treatment. *Carbohydrate Polymers, 62*, 130–136.

Theocaris, P. S., & Spathis, G. D. (1982). Glass-transition behavior of particle composites modeled on the concept of interphase. *Journal of Applied Polymer Science, 27*, 3019–3025.

Wetzel, B., Haupert, F., & Zhang, M. Q. (2003). Epoxy nanocomposites with high mechanical and tribological performance. *Composites Science and Technology, 63*, 2055–2067.

Yuen, S. (1974). Pullulan and its applications. *Process Biochemistry, 9*, 7–9, 22.

Zhu, A. J., & Sternstein, S. S. (2003). Nonlinear viscoelasticity of nanofilled polymers: interfaces, chain statistics and properties recovery kinetics. *Composites Science and Technology, 63*, 1113–1126.